

Available online at www.sciencedirect.com

ScienceDirect

journal homepage: www.elsevier.com/locate/dental

Tailoring the biologic responses of 3D printed PEEK medical implants by plasma functionalization

Xingting Han^{a,b,*}, Neha Sharma^{c,d}, Sebastian Spintzyk^{b,e},
Yongsheng Zhou^a, Zeqian Xu^{b,f}, Florian M. Thieringer^{c,d,1},
Frank Rupp^{b,*,1}

^a Department of Prosthodontics, Peking University School and Hospital of Stomatology, National Center of Stomatology, National Clinical Research Center for Oral Diseases, National Engineering Laboratory for Digital and Material Technology of Stomatology, Beijing Key Laboratory of Digital Stomatology, NHC Key Laboratory of Digital Technology of Stomatology, 22 Zhongguancun Avenue South, Haidian District, Beijing 100081, PR China

^b University Hospital Tübingen, Section Medical Materials Science and Technology, Oslanderstr. 2-8, Tübingen D-72076, Germany

^c Medical Additive Manufacturing Research Group, Hightech Research Center, Department of Biomedical Engineering, University of Basel, Allschwil, Switzerland

^d Department of Oral and Cranio-Maxillofacial Surgery, University Hospital Basel, Basel, Switzerland

^e ADMiRE Lab - Additive Manufacturing, intelligent Robotics, Sensors and Engineering, School of Engineering and IT, Carinthia University of Applied Sciences, Villach, Austria

^f Department of Prosthodontics, Shanghai Ninth People's Hospital, Shanghai Jiao Tong University School of Medicine; College of Stomatology, Shanghai Jiao Tong University; National Center for Stomatology; National Clinical Research Center for Oral Diseases; Shanghai Key Laboratory of Stomatology; Shanghai Engineering Research Center of Advanced Dental Technology and Materials, Shanghai, PR China

ARTICLE INFO

Article history:

Received 22 November 2021

Received in revised form 20 April 2022

Accepted 27 April 2022

ABSTRACT

Objective: The objective of this study was to determine the effect of two plasma surface treatments on the biologic responses of PEEK medical implants manufactured by fused filament fabrication (FFF) 3D printing technology.

Methods: This study created standard PEEK samples using an FFF 3D printer. After fabrication, half of the samples were polished to simulate a smooth PEEK surface. Then, argon (Ar) or oxygen (O₂) plasma was used to modify the bioactivity of FFF 3D printed and po-

* Corresponding author at: Department of Prosthodontics, Peking University School and Hospital of Stomatology, National Center of Stomatology, National Clinical Research Center for Oral Diseases, National Engineering Laboratory for Digital and Material Technology of Stomatology, Beijing Key Laboratory of Digital Stomatology, NHC Key Laboratory of Digital Technology of Stomatology, 22 Zhongguancun Avenue South, Haidian District, Beijing 100081, PR China

** Corresponding author.

E-mail addresses: xingtinghan@126.com, xingtinghan@bjmu.edu.cn (X. Han), neha.sharma@unibas.ch (N. Sharma), s.spintzyk@fh-kaernten.at (S. Spintzyk), kqzhouysh@hsc.pku.edu.cn (Y. Zhou), xuzeqian934130@126.com (Z. Xu), florian.thieringer@usb.ch (F.M. Thieringer), frank.rupp@med.uni-tuebingen.de (F. Rupp).

¹ These authors contributed equally to this work.

<https://doi.org/10.1016/j.dental.2022.04.026>

0109-5641/© 2022 The Author(s). Published by Elsevier Inc. on behalf of The Academy of Dental Materials.

CC_BY_NC_ND_4.0

Keywords:

Polyetheretherketone
Fused Filament Fabrication
Plasma surface treatment
Wettability
Bioactivity

lished PEEK samples. Scanning electron microscopy (SEM) and a profilometer were used to determine the microstructure and roughness of the sample surfaces. The wettability of the sample surface was assessed using a drop shape analyzer (DSA) after plasma treatment and at various time points following storage in a closed environment. Cell adhesion, metabolic activity, proliferation, and osteogenic differentiation of SAOS-2 osteoblasts were evaluated to determine the *in vitro* osteogenic activity.

Results: SEM analysis revealed that several spherical nanoscale particles and humps appeared on sample surfaces following plasma treatment. The wettability measurement demonstrated that plasma surface treatment significantly increased the surface hydrophilicity of PEEK samples, with only a slight aging effect found after 21 days. Cell adhesion, spreading, proliferation, and differentiation of SAOS-2 osteoblasts were also up-regulated after plasma treatment. Additionally, PEEK samples treated with O₂ plasma demonstrated a higher degree of bioactivation than those treated with Ar.

Significance: Plasma-modified PEEK based on FFF 3D printing technology was a feasible and prospective bone grafting material for bone/dental implants.

© 2022 The Author(s). Published by Elsevier Inc. on behalf of The Academy of Dental Materials.

CC_BY_NC_ND_4.0

1. Introduction

Polyetheretherketone (PEEK) is a high-temperature thermoplastic used as a bone reconstruction material for cranio-maxillofacial and orthopedic surgeries [1–3]. In dental applications, PEEK is gaining attracting attention as dental implants and prostheses [4]. This polymer is a semi-crystalline material with high thermal stability, mechanical properties, good chemical, and sterilization resistance [5,6]. In addition, PEEK exhibits good biocompatibility, non-toxicity and is radiolucent with magnetic resonance imaging compatibility [7–11]. In contrast to metals such as titanium (Ti), PEEK has a relatively low elastic modulus (Ti: 102–110 GPa; PEEK: 3–4 GPa), which is closer to human cortical bone (14 GPa) [2,12]. This characteristic property helps to reduce the stress shielding effect at the bone-implant interface, thereby minimizing implant loosening and peri-implant bone loss [13]. Despite many advantages, PEEK is bioinert with low surface energy, promoting fibrosis formation and hindering it from binding to bones [14]. The fibrous tissue formation around PEEK implants is due to reduced osteoblastic differentiation of progenitor cells and production of an inflammatory environment that favors cell death via apoptosis and necrosis [15]. This surface inertness does not account for appropriate interfacial bioactivity [16]. Thus, proper strategies should be identified to improve the bioactivity of PEEK to realize its potential benefits.

Several surface modification strategies have been carried out to activate PEEK implant surfaces to enhance osseointegration properties through coatings and direct surface treatments [17–19]. Various materials have been deposited on the surface of PEEK, including hydroxyapatite (HA), Ti, and titanium dioxide (TiO₂), and a significant increase in bioactivities of PEEK materials could be detected after applying these bioactive coatings [20,21]. However, the load-bearing capacity was reduced with HA as the fatigue-life of HA-coated PEEK was dependent on HA content and applied load [22]. Although this drawback was not noted with Ti, the clinical success of these coatings may be limited due to their potential instability and delamination in physiological or surgical environments [23]. Besides applying coatings, one important

direct surface treatment is plasma surface treatment, which provides an alternative to traditional methods by wet chemical cleaning, cross-linking, and etching [4,24]. This treatment is economical that does not alter PEEK bulk properties. Previous studies data indicate that activation of PEEK with plasma treatment results in improved *in vitro* cell adhesion, proliferation, osteoblast differentiation, and *in vivo* bone-implant interface stability and osseointegration compared to the pristine PEEK. [9,13,25,26]. However, the hydrophilic surface generated by plasma treatment is temporary. After a few hours to a few days of exposure to ambient air, the functionalized surface created by plasma treatment might be buried beneath the polymer surface. Therefore, the method of storing plasma-treated samples is critical for medical implants. Besides, most previous studies utilized polished PEEK as a substrate fabricated with traditional manufacturing processes, e.g., injection molding, to analyze the effects of plasma treatment. Tailoring effects of plasma treatment on 3D printed PEEK implants is still unknown.

In the last few decades, additive manufacturing (AM, also known as 3D printing) has become an essential technology for fabricating medical implants with complex geometries [27]. The outstanding advantage of AM is the ability to form shapes that cannot be formed with traditional manufacturing methods. Avoiding design constraints, mass customization, and lesser waste generation are hallmarks of AM [28]. Due to the ability to fabricate customized products quickly, 3D printing is increasingly utilized in medical applications to fabricate patient-specific implants [29,30]. Among different 3D printing technologies, fused filament fabrication (FFF, also called fused deposition modeling, FDM) is one of the most popular and fastest-growing technologies [31,32]. 3D printing of PEEK using FFF is a recent technology that allows fast, cost-effective, and in-house fabrication of PEEK implants [33,34]. Due to the layer-by-layer fabrication mechanism in FFF, 3D printed PEEK implants exhibit a specific surface topography, in contrast to the smooth surface of the injection-molded or milled traditional PEEK implants [35]. Our previous work reported the feasibility of characteristic surface topographies comprising roughened surfaces and anisotropic printing

structures (peaks and valleys) on FFF 3D printed PEEK implants [8,12]. These surface topographies, integral to the FFF fabrication mechanism, can play an essential role in stimulating the bioactivity potential of FFF 3D printed PEEK implants [8,12]. Therefore, investigating the impact of plasma surface treatment on the biological behavior of 3D printing PEEK materials is a promising method for fully utilizing the benefits of PEEK materials and 3D printing technologies and the production and design of new bone reconstruction materials.

In the present work, FFF 3D printed PEEK samples were oxygen (O₂) and argon (Ar) plasma-treated to determine surface activation conditions for cell adhesion, spreading, metabolic activity, proliferation, and differentiation. To reduce the aging effect associated with plasma surface treatment and to extend the use of plasma modification in bone scaffolds, we stored plasma-treated samples in a closed environment and measured the surface wettability at various time points. We hypothesize that plasma treatment can be successfully applied to FFF 3D printed PEEK implants and holds relative importance for suitable in vitro osteogenic and biologic responses.

2. Materials and methods

2.1. Specimen fabrication

A total of 288 biomedical grade disk PEEK standard samples, with dimensions of 14 mm diameter and 2 mm thickness, were fabricated using an FFF 3D printer (Apium P220, Apium Additive Technologies GmbH, Karlsruhe, Germany). Table 1 lists the printing parameters used for the fabrication process. The filament used was a medical-grade PEEK 3D filament (Evonik VESTAKEEP®i4 G resin, Evonik Industries AG, Essen, Germany, Table A.1). Prior to printing, a special fixative spray (DimaFix, DIMA 3D, Valladolid, Spain) was applied on the print bed to achieve adequate adhesion of samples. Later, the FFF 3D printed PEEK samples were further divided into two groups: without polishing and with polishing. For the polished group, specimens were modified with a grinding machine (Buehler, Coventry, UK) using series of SiC abrasive papers with an increasing grit number (P1200, P2500, and P4000, Buehler, Lake Bluff, IL, USA). Table A.2 shows the thickness of FFF 3D printed PEEK before and after polishing (n = 5 per group).

2.2. Plasma treatment

Before plasma treatment, PEEK samples were ultrasonically cleaned with distilled water and 70% ethanol (15 min for each) and then dried with nitrogen for 20 s. To activate PEEK samples, argon (Ar) and oxygen (O₂) plasma treatments were used (DENTAPLAS PC, Diener electronic GmbH, Ebhausen, Germany). PEEK specimens were placed on a metal drawer in the plasma chamber. Subsequently, the chamber was evacuated and flushed with Ar and O₂ gases, respectively. A 15 min plasma treatment duration was chosen based on previous publications [36,37]. Other parameters were as follows: pressure: 100 Pa, distance: 50 mm, power output: 100 W,

Table 1 – Printing parameters of FFF 3D printed PEEK.

Printing parameters	Value
Layer thickness	200 μm
Nozzle diameter	0.4 mm
Printing speed	2000 mm/min
Raster angle	+ 45°/–45°
Print head temperature	480 °C
Print bed temperature	130 °C

frequency: 40 kHz, and flow rate: Ar: 51 sccm; O₂: 16 sccm. Fig. 1 exhibits the group classification and experimental process. Fig. A.1 shows the FFF 3D printed and polished PEEK samples before and after plasma treatments. Before conducting the subsequent experiments, all PEEK specimens in each group were ultrasonically cleaned and sterilized with 70% ethanol (15 min), then dried in a sterile workbench (Heraeus, Hanau, Germany) for 20 min

2.3. Surface characterization

Surface microstructures on FFF 3D printed and polished PEEK sample surfaces (n = 2 per group) were investigated with scanning electron microscopy (SEM, LEO 1430, Zeiss, Oberkochen, Germany) at a magnification of 10,000×, both before and after Ar and O₂ plasma treatments. Before surface observation, PEEK specimens were coated with Au-Pd (20 nm) (SCD 050, Baltec, Lübeck, Germany).

Surface roughness of 3D printed and polished PEEK before and after plasma treatment was analyzed by a profilometer (Perthometer Concept S6P, Mahr, Göttingen, Germany, n = 4 per group, test area: 3 mm × 3 mm, test profiles: 121). 3D roughness parameters of arithmetic mean height (Sa) and root mean square height (Sq) were calculated by the corresponding software (MountainsMap Universal 7.3, Digital Surf, Besançon, France).

The surface wettability of PEEK specimens in different groups (n = 4 per group) was evaluated by determining the water contact angle (WCA) using a contact angle goniometer (Drop shape analyzer (DSA) 10-Mk 2, Krüss, Hamburg, Germany). Sessile drops of 2 μl ultrapure water were deposited on the PEEK samples' surfaces. After 20 s wetting, the contact angle was analyzed using the DSA calculation software (version 1.90.0.11, Krüss, Hamburg, Germany). To evaluate the aging on PEEK substrates after plasma treatment, samples were stored in a 24-well plate (Cluster, Corning, Tewksbury, MA, USA) under room temperature. The WCA was measured at 0, 1, 3, 7, 14 and 21 d, respectively. To reveal any influence of the sterilization process on the water contact angle, the WCA values were measured following plasma treatment and subsequent sterilization with 70% ethanol.

2.4. In vitro biological test

2.4.1. Cell culture

A human osteosarcoma cell line (SAOS-2 osteoblast, DSMZ GmbH, Braunschweig, Germany) was used for in vitro evaluation of cell adhesion, proliferation, and osteogenic

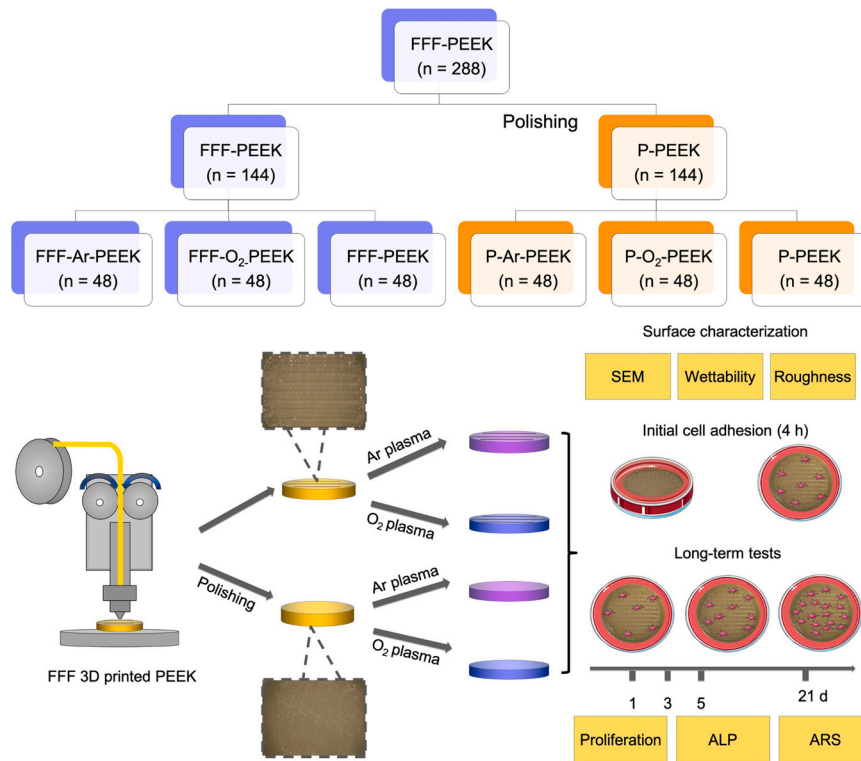


Fig. 1 – Schematic graph of grouping and experimental process. FFF-PEEK: FFF 3D printed PEEK; P-PEEK: polished PEEK; FFF-Ar-PEEK: FFF 3D printed PEEK treated by Ar plasma; FFF-O₂-PEEK: FFF 3D printed PEEK treated by O₂ plasma; P-Ar-PEEK: polished PEEK treated by Ar plasma; P-O₂-PEEK: polished PEEK treated by O₂ plasma; SEM: scanning electron microscopy; ALP: alkaline phosphatase activity; ARS: alizarin red staining.

differentiation potential. SAOS-2 osteoblasts were suspended in McCoy's 5 A medium (Sigma-Aldrich, Steinheim, Germany) supplemented with 15% fetal bovine serum (FBS, Life Technologies Co., Carlsbad, CA, USA), 1% L-glutamine (GlutaMAX, Life Technologies Co., Carlsbad, CA, USA) and 1% penicillin and streptomycin (15140–122, Life Technologies Co., Carlsbad, CA, USA). The cells were cultured in a cell incubator at a culturing temperature of 37 °C in an atmosphere of 5% CO₂ and 95% humidity. The culture medium was changed 24 h after seeding and was renewed twice a week. Prior to each test, sterilized PEEK disks were fixed on the bottom of a 24-well cell culture plate with sterile wax to avoid floating. All the biological tests were performed at least two times in independent experiments.

2.4.2. Initial cell adhesion

The inoculating density of SAOS-2 osteoblast cultured onto PEEK sample surfaces was 250,000 cells/ml in 1.2 ml McCoy's 5 A supplemented medium ($n = 4$ for each group). After a 4 h culturing time, cell adhesion on PEEK sample surfaces was measured by crystal violet staining. As there is a linear correlation, cell numbers can be indirectly determined by quantifying the optical density of the re-solubilized dye.

After 4 h incubation, the PEEK samples from each well were rinsed with 500 μ l Hank's balanced salt solution (HBSS, Biochrom AG, Berlin, Germany) to remove loosely attached cells. Next, the adhered cells were fixed with 500 μ l 3% paraformaldehyde solution (MERCK, Darmstadt, Germany) in

Dulbecco's phosphate-buffered saline (DPBS, without calcium and magnesium, Gibco, Paisley, UK) for 15 min. Then, each sample was stained by 500 μ l crystal violet dye for 15 min (Sigma-Aldrich, St. Louis, USA). After staining, each sample was rinsed with 500 μ l distilled water five times. Subsequently, the PEEK disks were photo-documented by a microscope (M400, Wild Heerbrugg, Gais, Switzerland) equipped with a digital camera (EOS 500D, Canon, Tokyo, Japan). Afterward, the crystal violet dye on each sample surface was solubilized with 600 μ l pure methanol (MERCK, Darmstadt, Germany) for 30 min. An ELISA reader measured the optical density (OD) values at 550 nm (Tecan Austria GmbH, Grödigg, Austria). The mean OD values of the background controls were subtracted from the corresponding groups.

2.4.3. Cell morphology and viability

A density of 50,000 cells/ml of SAOS-2 was inoculated on the sample surfaces from various groups ($n = 3$ per group) to observe cell morphology and viability. After 24 h incubation, cell attachment and spreading were determined by the SEM. Before observing, the adherent cells on the sample surfaces were fixed with 2% glutaraldehyde solution at 4 °C for 24 h and dehydrated using severe ethanol concentrations solution (30%, 40%, 50%, 60%, 70%, 80%, 90%, 96%, and 100%, 15 min for each concentration). Then the samples were further dehydrated by critical point drying (E3100, Quorum Technologies, Laughton, UK) with liquid CO₂. Before SEM

evaluation, PEEK sample surfaces were spattered with a 20 nm thick Au–Pd coating (SCD 050, Baltec, Lübeck, Germany).

The cell morphology and viability of SAOS-2 osteoblast were evaluated by live/dead fluorescence staining with a seeding density of 50,000 cells/ml ($n = 4$ per group). After 24 h incubation, the PEEK samples from each group were rinsed with HBSS. The staining solution was prepared by mixing HBSS, 25 $\mu\text{g/ml}$ FDA, and 1.25 $\mu\text{g/ml}$ EB (Sigma-Aldrich Chemie GmbH, Taufkirchen, Germany). After 10 min staining in darkness, the samples were rinsed with HBSS again and photo-documented by a microscope (Olympus, Tokyo, Japan) equipped with a 550D DSLR camera (Canon, Tokyo, Japan).

2.4.4. Cell metabolic activity and proliferation assay

The seeding density of SAOS-2 osteoblast for cell metabolic activity test was 50,000 cells/ml in 1.2 ml/well McCoy's 5 A supplemented medium in 24-well plate ($n = 4$ per group). After culturing for 1, 3, and 5 d, 1.2 ml of the original medium was removed and replenished with 0.6 ml fresh medium. Cell metabolic activity was determined by adding 60 μl cell counting kit-8 assay (CCK-8) labeling reagent (Dojindo Molecular Technologies, Inc., Rockville, MD, USA). After additional incubation for 2 h, the supernatant from each well was transferred to a new 96-well plate (4 wells for each sample, 100 μl per well). Then, the OD value of the supernatant was measured spectrophotometrically by the ELISA reader at 492 nm wavelength with the reference at 620 nm. Cell proliferation was examined indirectly by measuring the cell metabolic activity by CCK-8 assay at different time points (1, 3, and 5 d).

2.4.5. Alkaline phosphatase activity (ALP) assay

The seeding density for the ALP test was 50,000 cells/ml in 1.2 ml/well McCoy's 5 A supplemented medium in 24-well plate ($n = 4$ for each group). On the 4th day of incubation, the cell culture medium was replaced by an osteogenic inductive medium (McCoy's 5 A supplemented medium + 10 mM β -glycerophosphate, 4 μM dexamethasone, and 100 μM L-ascorbic acid, Sigma-Aldrich, St. Louis, USA). After an additional 24 h incubation, 1 ml 0.2% lysis solution (TritonX-100, MERCK, Darmstadt, Germany) was added to each well of the 24-well culture plate and incubated for 1 h. Before measuring the ALP activity, a standard concentration curve was made by diluting the solution of p-nitrophenol (Sigma-Aldrich, St. Louis, USA) and NaOH (MERCK, Darmstadt, Germany) with distilled water (Ampuwa, Fresenius Kabi Deutschland GmbH, Bad Homburg, Germany). The ALP activity was evaluated by p-nitrophenyl phosphate (pNPP, Sigma-Aldrich, St. Louis, USA) using the ELISA reader at 405 nm as a substrate. According to the manufacturing instructions, the ALP activity value was normalized by measuring the corresponding content of total protein by a micro BCA protein assay kit (Pierce, Thermo, USA). Therefore, the ALP activity was expressed as the corresponding protein content (μmol formed pNPP/min/mg protein).

2.4.6. Alizarin red staining (ARS) measurement

Mineralized nodule formation was considered to be an outcome for osteogenic maturation. In this study, the

mineralized depositions were evaluated by staining with ARS with a cell seeding density of 50,000 cells/ml ($n = 4$ for each group). During the cell culture period, the cell medium was changed twice a week. After 21 d incubation, the SAOS-2 cells attached to the sample surfaces were rinsed with DPBS two times and fixed with 3% paraformaldehyde in the DPBS. After fixation for 30 min, the paraformaldehyde was removed entirely, and cells were rinsed with DPBS three times. Subsequently, the cells attached to the sample surfaces were stained with 40 mM ARS ($\text{pH} = 4.2$, Sigma-Aldrich, St. Louis, USA) under mild shaking in the incubator. After staining for 30 min, the excess ARS was eliminated using distilled water 4 times with gentle shaking. The stained mineralized nodules on the sample surfaces were photo-documented by photomicroscopy. Afterward, 0.5 M hydrogen chloride (HCL, MERCK, Darmstadt, Germany) supplemented with 5% sodium dodecyl sulfate (SDS, Sigma-Aldrich, St. Louis, USA) was used to elute the staining for 30 min with mild shaking. The ELISA reader was used to evaluate the intensity of ARS staining at 405 nm wavelength. The mean OD values of the background controls were subtracted from the corresponding groups.

2.5. Statistical analysis

Unless otherwise indicated, all the data are expressed as mean \pm standard deviations. The software SPSS Version 25 (SPSS INC, Chicago, IL, USA) was used for data analysis. Before comparing the means, the data distribution and homogeneity of variances were analyzed using the Shapiro-Wilk and Levene tests. One-way analysis of variance (ANOVA) followed by Tukey post-hoc test was used for the data with normal distribution and homogeneity of variances. The nonparametric analysis of Kruskal–Wallis followed by Dunn's multiple comparisons test was used for the data non-normality or nonhomogeneity of variances.

3. Results

3.1. Characterization of surface microstructures

Fig. 2 shows SEM images of FFF 3D printed and polished PEEK with and without plasma surface treatments under 10,000 \times magnification. The native FFF-PEEK showed a relatively smooth and homogenous surface. On the other hand, for native P-PEEK samples, after polishing, the printing structures inside the PEEK material were disclosed on the sample surfaces. After Ar and O₂ plasma treatment, some spherical nanoscale particles (white spots) appeared on FFF 3D printed and polished PEEK surfaces. Moreover, in both groups, a combination of micro- and nano-scale hybrid structures was observed after plasma treatment.

3.2. Surface roughness

Surface roughness and morphology before and after plasma treatment are illustrated in Fig. 3. The result indicated that the FFF 3D printed PEEK showed significantly rougher surfaces than the polished samples (Sa: FFF-Ar-PEEK: 8.55 \pm 1.42 μm ; FFF-O₂-PEEK: 9.26 \pm 2.44 μm ; FFF-PEEK: 8.72

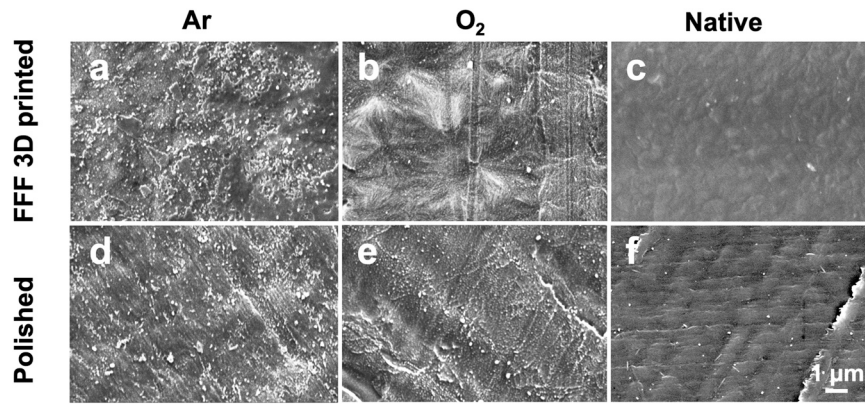


Fig. 2 – SEM images of FFF 3D printed and polished PEEK before and after Ar and O₂ plasma treatment under 10,000 × magnification. (a) FFF-Ar-PEEK; (b) FFF-O₂-PEEK; (c) FFF-PEEK; (d) P-Ar-PEEK; (e) P-O₂-PEEK; (f) P-PEEK.

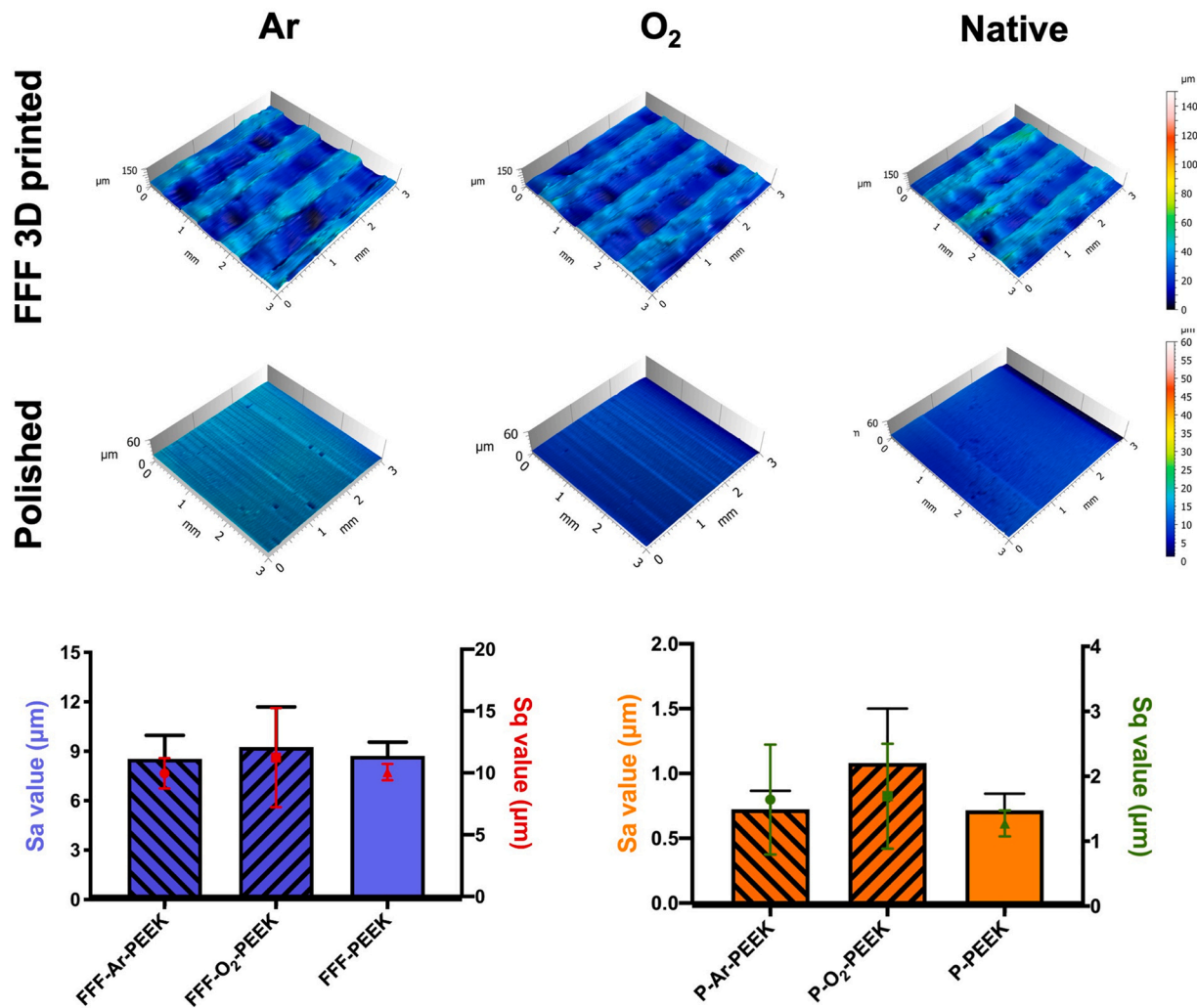


Fig. 3 – Reconstructed 3D surface topographies: (a) FFF-Ar-PEEK; (b) FFF-O₂-PEEK; (c) FFF-PEEK; (d) P-Ar-PEEK; (e) P-O₂-PEEK; (f) P-PEEK. (g) and (h): Sa and Sq values of FFF 3D printed and polished PEEK samples. The data are presented as means ± standard deviation.

$\pm 0.83 \mu\text{m}$; P-Ar-PEEK: $0.72 \pm 0.14 \mu\text{m}$; P-O₂-PEEK: $1.08 \pm 0.42 \mu\text{m}$; P-PEEK: $0.72 \pm 0.13 \mu\text{m}$. Sq: FFF-Ar-PEEK: $9.96 \pm 1.22 \mu\text{m}$; FFF-O₂-PEEK: $11.23 \pm 4.00 \mu\text{m}$; FFF-PEEK: $10.07 \pm 0.66 \mu\text{m}$; P-Ar-PEEK: $1.64 \pm 0.85 \mu\text{m}$; P-O₂-PEEK: $1.69 \pm 0.81 \mu\text{m}$; P-PEEK: $1.28 \pm 0.20 \mu\text{m}$). But within FFF 3D printed or polished groups, only a slight increase in roughness values could be detected after plasma treatment without statistical significance ($p > 0.05$).

3.3. Surface wettability

To evaluate surface wettability, water contact angle (WCA) of Ar and O₂ plasma-treated PEEK were measured at different time points (Fig. 4). Before plasma treatment, FFF 3D printed and polished PEEK surfaces were both hydrophobic with the WCA value of $90.4 \pm 7.4^\circ$ and $89.5 \pm 2.5^\circ$, respectively. It was noticed that after Ar and O₂ plasma treatment, the WCA of FFF 3D printed and polished PEEK surfaces decreased significantly ($p < 0.0001$, FFF-Ar-PEEK: $35.7 \pm 13.0^\circ$, FFF-O₂-PEEK: $25.6 \pm 8.8^\circ$, P-Ar-PEEK: $41.1 \pm 7.3^\circ$, and P-O₂-PEEK: $38.0 \pm 3.1^\circ$). As the storage time increased, the WCA showed a gentle increase with a final stable value below 60° after 21 d.

The effect of the sterilization process on the WCA values after plasma treatments is shown in Fig. A.2. The results revealed that ethanol sterilization significantly increased contact angles in both Ar and O₂ plasma-treated samples ($p < 0.0001$, before sterilization: FFF-Ar-PEEK: $1.1 \pm 2.1^\circ$, FFF-O₂-PEEK: $1.5 \pm 2.9^\circ$, P-Ar-PEEK: $1.8 \pm 3.6^\circ$, and P-O₂-PEEK: $1.2 \pm 3.4^\circ$).

3.4. Initial cell adhesion

Initial cell adhesion is always deemed a marker for cell functions, influencing cell proliferation and in vivo bone integration. To better understand the initial cell viability, cell attachments on PEEK sample surfaces after 4 h incubation were detected by crystal violet staining (Fig. 5). For FFF 3D printed PEEK, the samples treated with Ar and O₂ plasma indicated an increase in cell density than the native FFF-PEEK, especially for the O₂ plasma-treated group ($p < 0.05$). As for the polished samples, there was no significant difference in cell adhesion before and after plasma treatment ($p > 0.05$).

3.5. Cell morphology and viability

The SEM result of SAOS-2 osteoblast morphology, spreading, and intercellular connections were presented in Fig. 6. Before plasma surface treatment, the cells attached to the unmodified PEEK surfaces were sparse and showed a round morphology with a few pseudopodia. After Ar and O₂ plasma surface treatment, a significantly higher cell density on PEEK sample surfaces could be detected (FFF 3D printed groups: Ar and O₂: $p < 0.001$, polished groups: O₂: $p < 0.05$). Besides, the cells attached to the plasma-treated PEEK spread better compared with the unmodified samples with a fusiform and flat morphology. The SAOS-2 osteoblast displayed more visible pseudopodia for the plasma-treated PEEK samples.

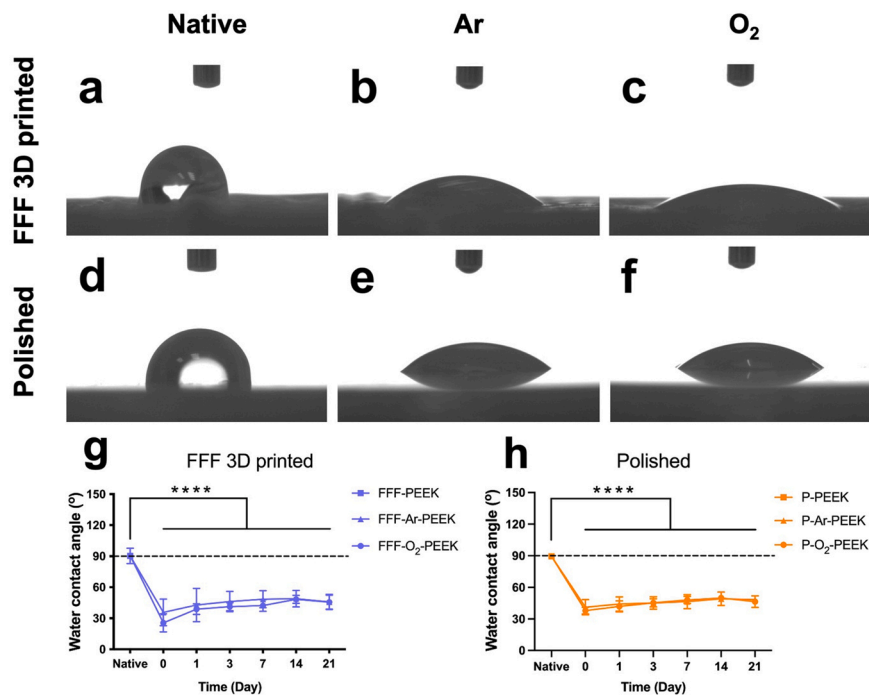


Fig. 4 – WCA measurements of FFF 3D printed and polished PEEK before and at different time points (0, 1, 3, 7, 14, and 21 d) after plasma treatment. (a)–(f): WCA of PEEK samples in different groups before and after Ar and O₂ plasma treatment; (a) FFF-PEEK; (b) FFF-Ar-PEEK; (c) FFF-O₂-PEEK; (d) P-PEEK; (e) P-Ar-PEEK; (f) P-O₂-PEEK; (g) and (h) quantitative results of WCA values for FFF 3D printed and polished PEEK samples before and after various plasma treatment time points. The dotted line represents the boundary of 90° between hydrophilicity and hydrophobicity, **** $p < 0.0001$.

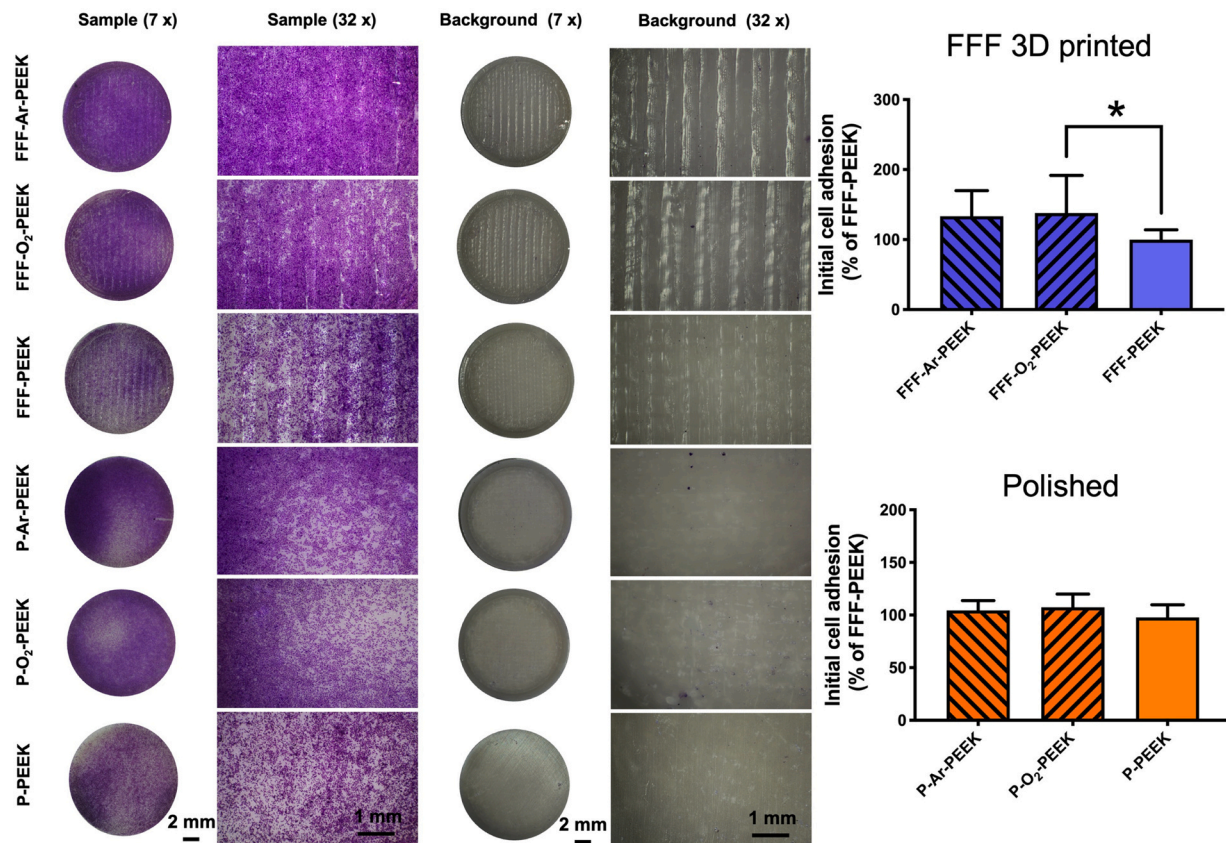


Fig. 5 – The qualitative and quantitative result of initial cell adhesion after 4 h incubation. The microscopic images indicate the stained SAOS-2 cells attached to the sample surfaces after 4 h incubation with a seeding density of 250,000 cells/ml under 7 × and 32 × magnification. The relative initial cell adhesion referred to the FFF-PEEK group, and the reference native FFF-PEEK was set to 100%. The data is represented in means ± standard deviations, * $p < 0.05$.

Fig. 7. shows the fluorescence microscopy images of cell viability, attachment, and spreading for the FFF 3D printed and polished PEEK groups before and after plasma surface treatment. After Ar and O₂ plasma treatment, the cell density attached to the sample surfaces was increased, both for FFF 3D printed and polished PEEK groups. Moreover, after Ar and O₂ plasma treatment, sample surface cell coverage enhanced significantly compared with the native FFF 3D printed and polished PEEK samples ($p < 0.0001$). The cells attached to the plasma-treated sample surfaces seemed to be more viable and stretchable compared with the native PEEK, both for the FFF 3D printed and polished groups.

3.6. Cell metabolic activity and proliferation

After incubation for 1, 3, and 5 d, the cell metabolic activity and proliferation were determined by CCK-8. Fig. 8 shows the cell metabolic activity of PEEK samples in various groups. After 1 d incubation, there was no significant difference in cell metabolic activity between the samples with and without plasma treatment, both for the FFF 3D printed and polished PEEK. After 3 d cultivation, for the FFF 3D printed samples, plasma-treated PEEK indicated increased cell metabolic activity, especially for the O₂ plasma-treated samples ($p < 0.05$). While for the polished PEEK groups, after 3 d incubation, the

increase in cell metabolic activity was still not significant after plasma treatments ($p > 0.05$). A similar trend could be observed after 5 d incubation.

3.7. Alkaline phosphatase activity (ALP) assay

Results of ALP activity evaluating the osteogenic differentiation are shown in Fig. 9. At the end of 5 d, the ALP activity for Ar and O₂ plasma-treated groups was slightly higher compared with the unmodified PEEK, but without statistical significance ($p > 0.05$), both for the FFF 3D printed and polished PEEK groups.

3.8. Alizarin red staining (ARS) measurement

Results of mineralized nodules formation showing the osteogenic mineralization are displayed in Fig. 10. For the FFF 3D printed PEEK groups, after plasma treatment of Ar and O₂, an increase in mineralized nodules could be detected compared with the untreated PEEK samples, especially for the O₂ plasma-treated group ($p < 0.05$). Besides, the optical microscope images of the FFF-Ar-PEEK and FFF-O₂-PEEK showed more positive and brighter red staining than the untreated PEEK. Similar to the FFF 3D printed PEEK groups, the P-O₂-PEEK also indicated more calcium phosphate deposits than

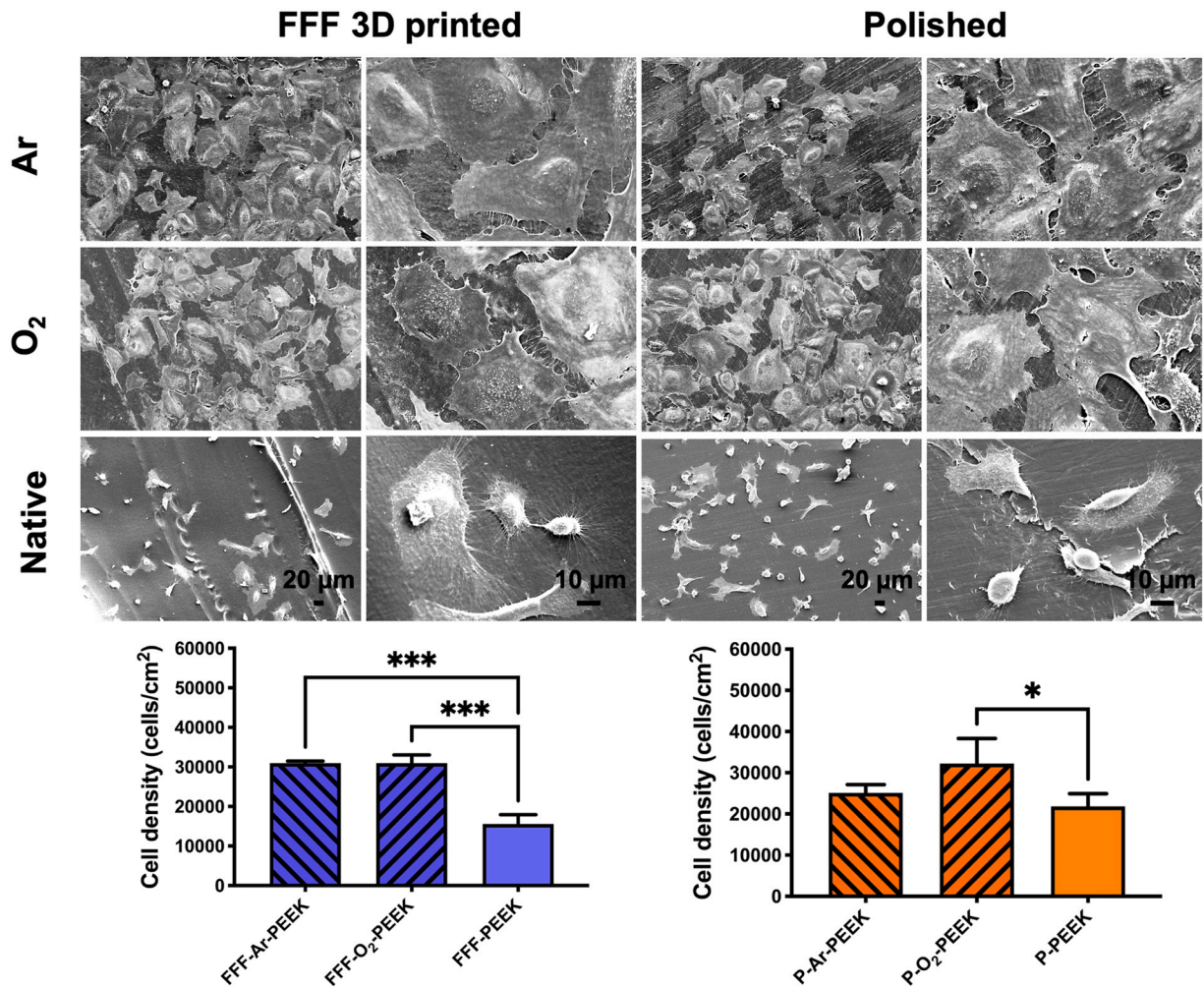


Fig. 6 – The qualitative and quantitative SEM results of SAOS-2 osteoblast morphology spread on FFF 3D printed and polished PEEK surfaces before and after plasma treatment. SEM images were taken after 24 h incubation under different magnification of 200 × and 1000 ×. The resulting cell density was quantified using the ImageJ software. Results were averaged from at least 6 200 × images. The data is represented in means ± standard deviations, * $p < 0.05$, *** $p < 0.001$.

the native P-PEEK samples ($p < 0.01$). Compared with the native P-PEEK group, more mineralized extracellular matrix deposition appeared on P-Ar-PEEK and P-O₂-PEEK sample surfaces.

4. Discussion

Plasma is a cost-effective and feasible way to enhance the bioactivity of PEEK and its composites. Nonetheless, research on its influence on 3D printed PEEK is still lacking. This study indicated that plasma surface treatment could tailor the biologic responses of FFF 3D printed and polished PEEK, including cell adhesion, metabolic activity, proliferation, and osteogenic differentiation. The mechanism thereof might be explained by surface microstructure, wettability, and chemical composition.

First, surface morphology and roughness could influence the bioactivity of PEEK material, as confirmed in numerous previous studies, and rough surfaces could promote initial

cell adhesion within a certain range [39]. In the present study, the SEM result (Fig. 2) indicated that the spherical nanoscale particles and humps appeared on sample surfaces after plasma treatment might be explained by the polymer chain broken due to the energetic ions [13]. The combination of micro- and nano-scale hybrid structures might influence the sample bioactivity and cellular behavior. Although the surface morphologies of the FFF 3D printed and polished PEEK groups changed, there was no significant difference in surface roughness following plasma treatment (Fig. 3). Fu et al. analyzed different plasma types on the physical, chemical, and biological surface properties of polished PEEK and got a similar result with this research that plasma treatment would not change the surface roughness significantly [4].

Second, surface wettability is another factor affecting cellular behavior. In this study, after plasma treatment, the wettability of the sample surface increased significantly, both for the FFF 3D printed and polished PEEK groups (Fig. 4). To a certain extent, the material's increased hydrophilicity stimulates osteoblast adhesion, proliferation, and differentiation on the

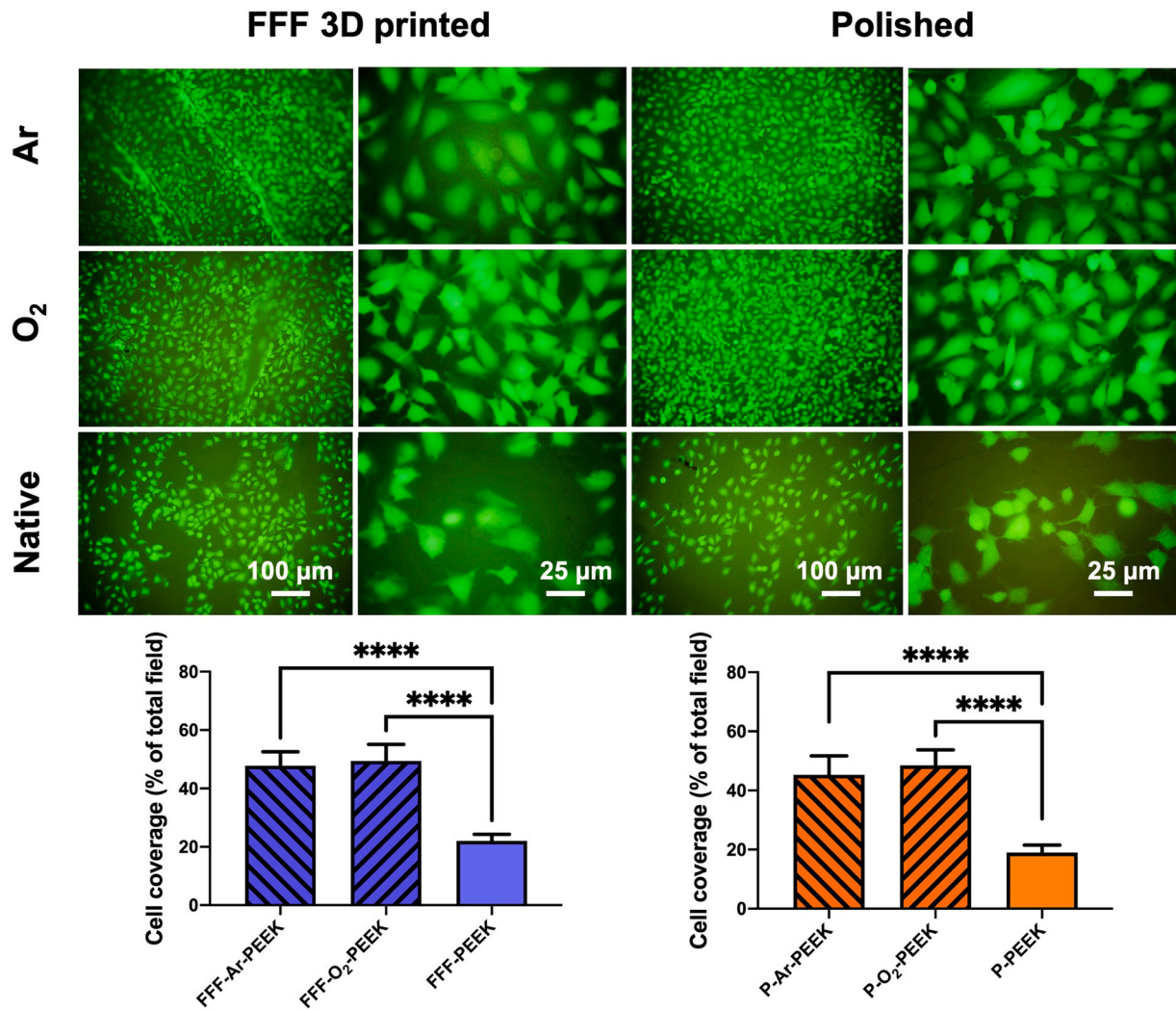


Fig. 7 – The qualitative and quantitative live/dead staining result of SAOS-2 osteoblast after 24 h incubation under 100 × and 400 × magnification. The green fluorescence indicated the live cells stained by FDA, and the dead cells stained by EB could not be detected in this experiment. The resulting cell coverage was quantified using the ImageJ software. Results were averaged from at least 6 100 × images. The data is represented in means ± standard deviations, **** $p < 0.0001$. (For interpretation of the references to colour in this figure legend, the reader is referred to the web version of this article.)

surface, which is favorable for bone formation following implantation [38]. Theoretically, substrates with high surface energy are more accessible to be wetted than those with low surface energy [39]. Since most polymers show low surface energy, they are insufficiently wetted by aqueous liquids. After plasma surface treatment, the surface properties, especially the surface wettability and energy, could be tailored. Plasma can activate the surface by the electric arc and provide valence electrons to bind liquid molecules [40]. Novotna et al. and Wang et al. used Ar plasma to modify PEEK surfaces and found increased surface wettability as well as changes in its surface chemistry [9,13]. In addition, Sundriyal et al. and Rochford et al. found similar patterns of increased surface wettability with O₂ plasma-treated PEEK [36,41]. Such findings could be confirmed in our study that shows a significant decrease in WCA after plasma surface treatment.

Table 2 compares the WCA values derived in our research to those reported in earlier publications following Ar and O₂ plasma treatment. The results suggested that the wettability of the sample surface following plasma treatment might be influenced by the gases utilized, the processing parameters, and subsequent sterilizing processes. Fu et al. investigated the surface wettability of O₂ plasma-treated PEEK before and after sterilization and discovered that contact angles were significantly enhanced during isopropanol sterilization [4]. This conclusion corroborated our studies, which indicated that sterilization might decrease the surface wettability achieved by plasma treatment (Fig. A.2). Despite the reduced wettability of PEEK following sterilizing with ethanol, Ar and O₂ plasma treatment significantly increased its in vitro bioactivity, indicating that plasma-treated PEEK fabricated with 3D printing technology may be a suitable material for bone reconstruction.

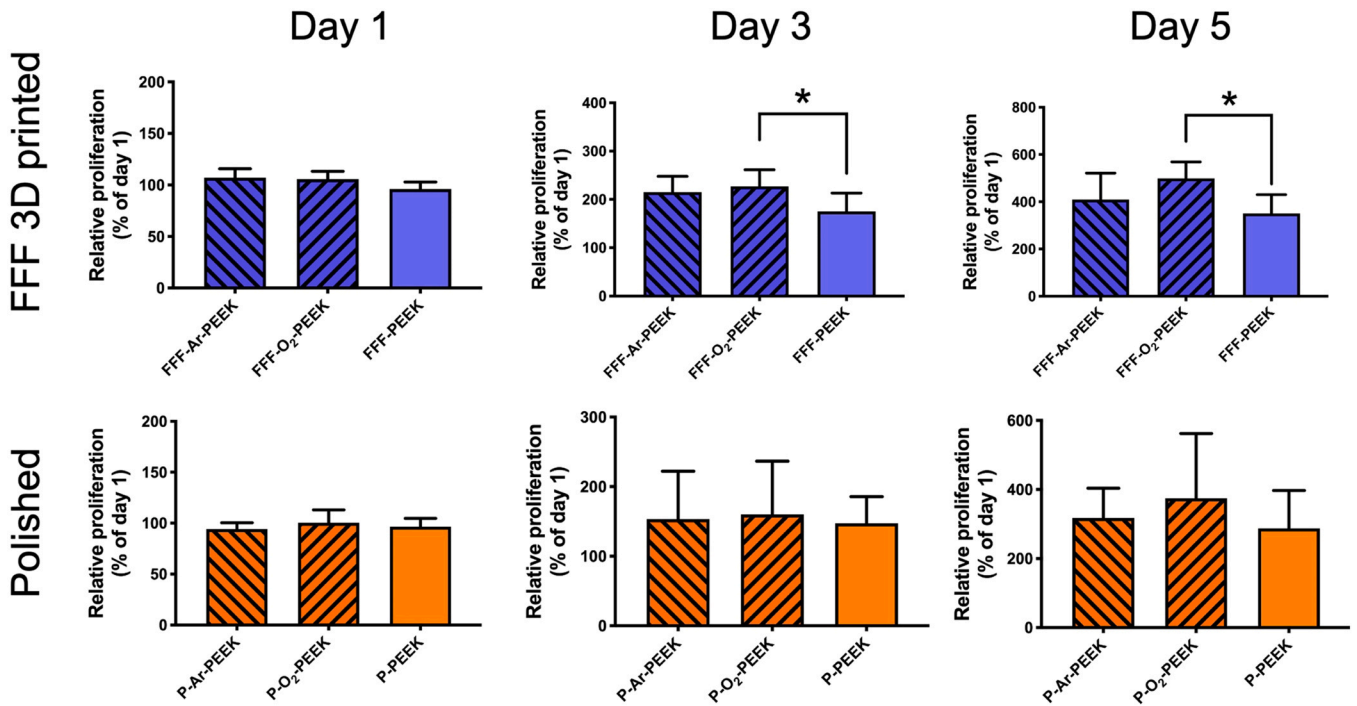


Fig. 8 – Relative cell metabolic activity and proliferation of SAOS-2 osteoblast on FFF 3D printed and polished PEEK samples with and without plasma surface treatment. The OD value of day 1 was used as the reference group and set to 100%. The data is represented in means \pm standard deviations, * $p < 0.05$.

After 21 d aging time, the samples saved in the 24-well plate indicated a slight aging effect. Compared with samples immediately after plasma treatment, the changes in the WCA were not significant (Fig. 4). In general, plasma-treated samples will experience a severe aging effect when exposed to ambient air, and the hydrophilicity will be reduced, even changes to be hydrophobic. Theoretically, the hydrophilic surface formed by plasma treatment is thermodynamically unstable, and the free energy gradient established at the

interface with the surrounding medium acts as a driving force, tending to decrease the surface energy while the treated object is stored in the air [13]. In this study, we evaluate the efficacy of storing plasma-treated PEEK samples in a closed environment to limit aging. As a result, the hydrophilic surface created by plasma treatment can be retained, which is believed to benefit the bioactivity of bone scaffolds [9,13]. Thus, preserving plasma-treated samples in a closed environment is an effective and practical method of

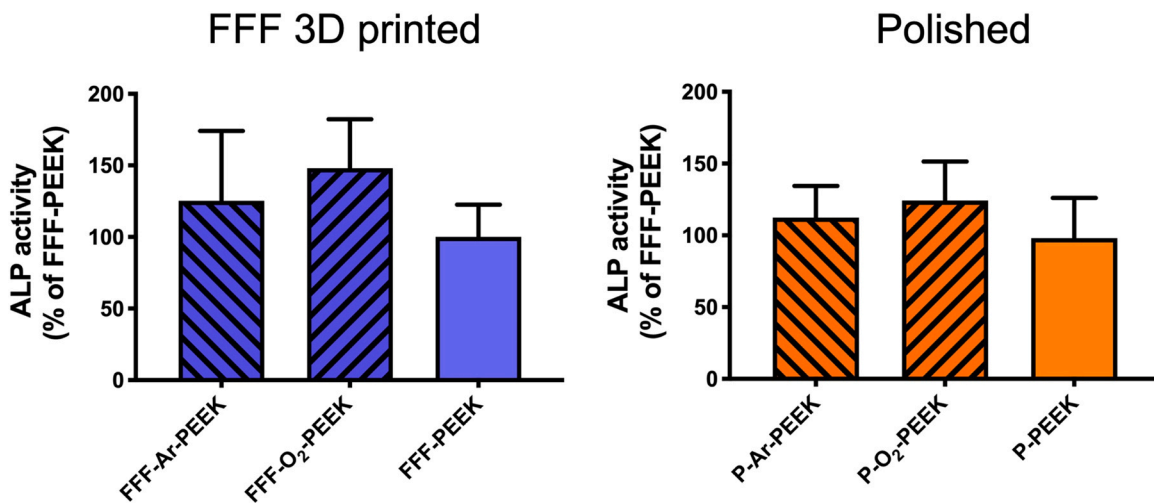


Fig. 9 – ALP activity of SAOS-2 osteoblast after 5 d incubation of FFF 3D printed and polished PEEK samples with and without plasma surface treatment. The data is represented in means \pm standard deviations.

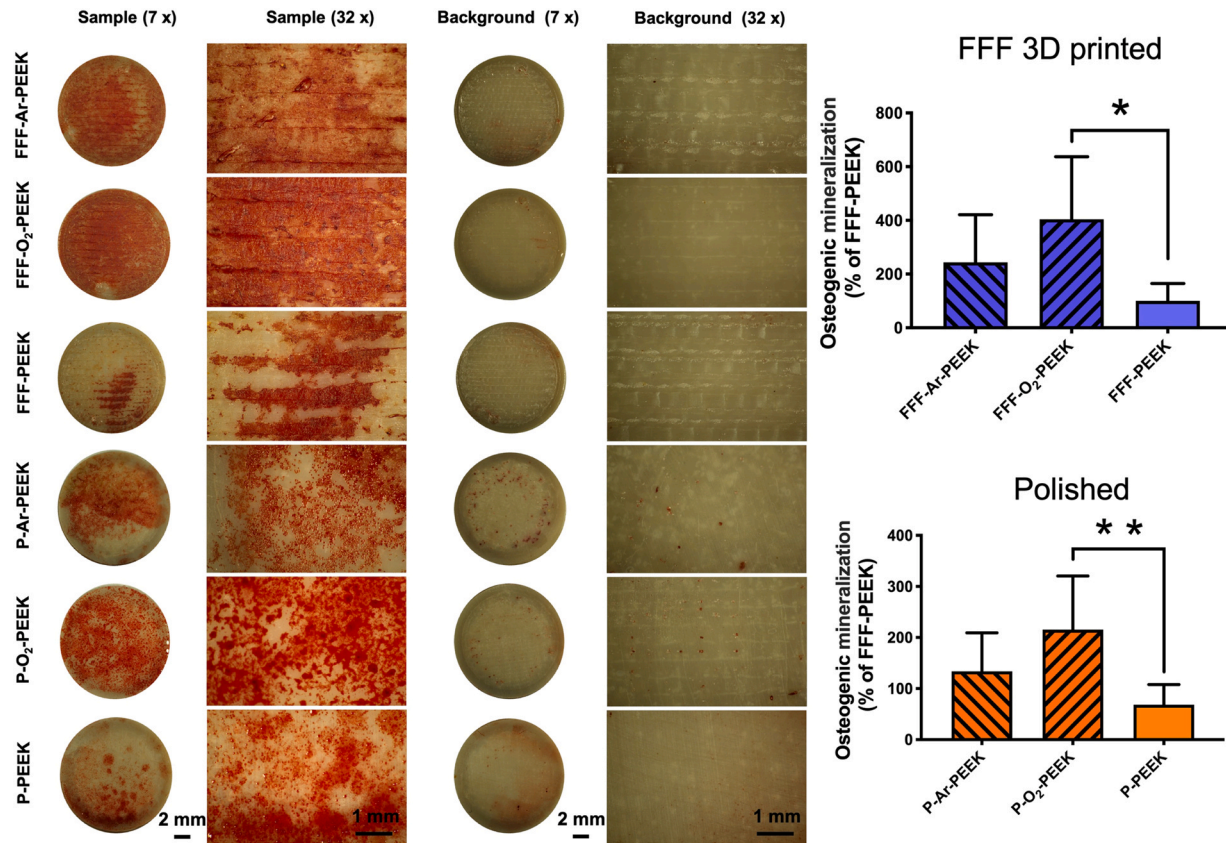


Fig. 10 – The qualitative and quantitative results of osteogenic differentiation after 21 d incubation. The microscopic images indicate the stained calcium phosphate deposits attached to the sample surfaces under 7 × and 32 × magnification. The relative osteogenic mineralization referred to the native FFF-PEEK, and the reference native FFF-PEEK group was set to 100%. The data is represented in means ± standard deviations, * $p < 0.05$, ** $p < 0.01$.

Table 2 – WCA values obtained from previous publications for Ar and O₂ plasma-treated PEEK samples.

Plasma gases	Time (min)	Power (W)	Sterilization steps after plasma	WCA (°)	Refs.
Ar	25	300	75% ethanol + UV light	66.40 ± 0.29	[24]
Ar/O ₂	35	200	No	2.4 ± 2.07	[42]
O ₂	30	200	No	Almost 0	[4]
O ₂ and Ar/O ₂	3	200	No	Almost 30	[43]
				O ₂ : 0.0 ± 0.0	
				Ar/O ₂ : 0.0 ± 0.0	
O ₂	1	200	No	O ₂ : 0.0 ± 0.0	[41]
				Ar/O ₂ : 2.8 ± 1.3	
				7 ± 1.24	
O ₂	15	/	Autoclave	53 ± 2	[36]
	30			51 ± 4	
Ar and O ₂	0.5–4	125	No	60–65	[44]
O ₂	15	45	Autoclave	60.0 ± 2.2	[37]
	30			59.0 ± 6.5	
Ar	60	300	75% ethanol	Almost 15	[13]
Ar	2	8.3	70% ethanol	23.2 ± 1.8	[9]
	4			21.8 ± 1.3	
	8			18.9 ± 1.7	
Ar/O ₂	5	10–200	70% ethanol	40–5	[26]

preventing bone scaffolds from aging and broadening the application of plasma surface modification in medical implants.

Finally, from the perspective of chemical composition, after plasma treatment, the surface chemical composition might be influenced by the used gas. Novotna et al. and Zhang et al. reported a significant increase in oxygen concentration following Ar plasma treatment [9,44]. However, Wang et al. discovered that when PEEK samples were treated with Ar plasma, the surface oxygen content reduced slightly [13]. On the other hand, Sundriyal et al. investigated the surface modification of O₂ plasma and discovered that the oxygen concentration increased from 14.8% to 48.9% following plasma treatment. Additionally, the percentage contributions of the C-OH/C-O-C group, C=O, and O=C-O groups, grew from 22.92 to 26.06, 0–18.97, and 0–16.9%, respectively [41]. Other studies also demonstrated that after O₂ plasma treatment, the surface oxygen content rose significantly [36,37,44]. Therefore, we speculated that Ar plasma might somewhat enhance the oxygen content, but its most significant effect would be mechanical cleaning by micro-sandblasting. While for the O₂ plasma, besides mechanical cleaning, it brought in the hydrophilic groups as well, which could stimulate osteoblast adhesion, proliferation, and osteogenic differentiation.

In this study, cell morphology and viability results indicated that compared with hydrophobic surfaces, cells prefer to attach and spread on the hydrophilic surfaces due to the enhanced binding ability between the substrate and extracellular matrix (ECM) proteins (Figs. 6 and 7) [25]. Besides, after plasma treatment, some nanoscale particles and humps appeared on the sample surfaces (Fig. 2). The hydrophilic nano-topographical surface could tailor the adhesion and spread of cells because of the enhancement in protein adsorption in the culture media [45]. Wang et al. and Xu et al. found that after Ar and O₂ plasma treatment, the cell attached to polished PEEK surfaces of each group indicated good viability, and cell density improved significantly with better spreading [13,25]. Similar findings were depicted in our results for polished groups. In addition, initial osteoblast adhesion experiments indicated that treatment with Ar and O₂ plasma had a minor effect on cell attachment, with the exception of the FFF-O₂-PEEK group (Fig. 5). This might be because, during the early stages of cell adhesion in 4 h, cells adhere primarily to sample surfaces by gravity. Some loosely attached cells were washed away during the following washing and staining processes. Therefore, there was no significant difference in initial cell adhesion before and after plasma treatment.

The long-term cell metabolic activity and proliferation test of SAOS-2 indicated that cells preferred to adhere and proliferate on the FFF 3D printed PEEK surfaces modified with O₂ plasma (Fig. 8), which might be related to the oxidized functional groups produced by O₂ plasma [41]. Some previous research found that following O₂ plasma treatment, the oxygen content of the sample surface increased and functional groups were introduced [37,41]. The addition of oxygen functional groups might alter the sample surface chemistry and charge and increase the binding ability of proteins,

thereby promoting metabolic activity and cell proliferation.

ALP activity is a crucial marker in the early stage of osteogenic differentiation. ALP participates in mature bone matrix calcification regulation and influences cell osteogenic mineralization ability [46]. In this study, the increase in ALP activity after plasma treatment was not significant, and only a gentle improvement could be observed (Fig. 9). Wang et al. treated polished PEEK samples with Ar and Ar + H₂O plasma and found out that after 14 d incubation, the ALP expression in the Ar + H₂O group increased significantly, whereas for the Ar plasma-treated PEEK, a slight decrease could be detected [13]. Xu et al. studied the influence of O₂ plasma treatment on polished PEEK bioactivities and found that higher levels of ALP production by cells could be detected on the plasma-treated samples than on the unmodified PEEK after 7 and 14 d incubation [25]. The mechanism for the influence of plasma surface treatment on ALP expression, which could be related to surface chemistry and nanosized surface features, is complex and not yet understood in detail [26]. After plasma surface treatment, hydrophilic functional groups and nanoscale features appeared on the sample surfaces (Fig. 2) [25]. Zhang et al. proved that the combination of micro- and nanoscale hybrid structures could improve osteoblast adhesion and differentiation [47]. These changes might contribute to increased ALP expression. In this study, we measured the ALP expression after 5 d incubation, and only a slight increase after plasma treatment could be detected. A long-term ALP activity could be measured at different time points (e.g., 7 and 14 d) to analyze the influence of plasma treatment on ALP expression in further studies.

Mineralized nodules formation is an index for osteoblast differentiation, which represents matrix maturation [48]. In this study, after 21 d incubation, the plasma-treated PEEK indicated higher levels of calcium phosphate deposits, especially for the O₂ plasma-treated PEEK (Fig. 10). A possible explanation for this finding is that after plasma treatment, a significant change in surface wettability was achieved. This hydrophilic bio-interface could form a suitable environment for bone nodule formation [40]. Besides, according to several previous publications, after O₂ plasma surface treatment, specific oxygen functional groups may be introduced to the sample surfaces, increasing osteoblast adhesion and differentiation and, as a consequence, the formation of mineralized nodules [41]. Therefore, compared with Ar plasma and native PEEK samples, O₂ plasma-treated groups demonstrated a significant enhancement in mineralized nodules formation.

Successful bone/dental implants require good biological activity and osseointegration. Osteoblast behavior is subtle and complex, and it can be influenced by a variety of factors, including the morphology, roughness, wettability, and chemical composition of the sample surface. These factors all have an effect on cell adhesion, proliferation, and differentiation. This research evaluated the effect of plasma treatment on FFF 3D printed PEEK and found a significant increase in *in vitro* osteogenic activity. In future studies, the plasma treatments' potential positive effect on the osseointegration of FFF 3D printed PEEK implants should be verified *in vivo*.

5. Conclusions

In this study, we combined plasma surface treatment and FFF 3D printing technology to generate micro/nano-topographical structures on the hydrophilic surface of PEEK utilized as a bone reconstruction material. Plasma treatment significantly improved the surface's hydrophilicity and changed the surface's morphology and roughness. In addition to the surface characterization alterations, plasma-treated PEEK with a hydrophilic and micro/nano-topographical surface induced in vitro SAOS-2 cell adhesion, metabolic activity, proliferation, and osteogenic differentiation. Besides, the effect of O₂ plasma on improving the biologic responses of PEEK samples is greater than that of Ar plasma treatment. More importantly, storing plasma-treated PEEK samples in a closed environment could decrease the aging effect, and the observed slight aging suggests chairside plasma treatments. These findings pave the way for plasma-treated PEEK implants based on the FFF 3D printing technology to be utilized in orthopedic and dental applications as a potential bone/dental implant material.

Funding

This research was supported by the National Natural Science Foundation of China (No. 82101073). The China Scholarship Council (CSC) is gratefully acknowledged for the financial support of Xingting Han (Grant 201606280045).

CRedit authorship contribution statement

Conceptualization, Sebastian Spintzyk and Frank Rupp; Formal analysis, Xingting Han; Methodology, Xingting Han, Neha Sharma, and Zeqian Xu; Project administration, Frank Rupp and Florian M. Thieringer; Writing – original draft, Xingting Han; Writing – review & editing, Xingting Han, Neha Sharma, Frank Rupp, Yongsheng Zhou, Florian M. Thieringer, and Sebastian Spintzyk.

Conflict of interest

The authors declare no conflict of interest.

Acknowledgments

The authors thank Ernst Schweizer for his assistance with the SEM analysis and Evi Kimmerle-Müller for her support in ALP and ARS tests.

Appendix A. Supporting information

Supplementary data associated with this article can be found in the online version at [doi:10.1016/j.dental.2022.04.026](https://doi.org/10.1016/j.dental.2022.04.026).

REFERENCES

- [1] Panayotov IV, Orti V, Cuisinier F, Yachouh J. Polyetheretherketone (PEEK) for medical applications. *J Mater Sci Mater Med* 2016;27. <https://doi.org/10.1007/s10856-016-5731-4>
- [2] Najeeb S, Zafar MS, Khurshid Z, Siddiqui F. Applications of polyetheretherketone (PEEK) in oral implantology and prosthodontics. *J Prosthodont Res* 2016;60:12–9. <https://doi.org/10.1016/j.jpor.2015.10.001>
- [3] Gao C, Wang Z, Jiao Z, Wu Z, Guo M, Wang Y, et al. Enhancing antibacterial capability and osseointegration of polyetheretherketone (PEEK) implants by dual-functional surface modification. *Mater Des* 2021;205. <https://doi.org/10.1016/j.matdes.2021.109733>
- [4] Fu Q, Gabriel M, Schmidt F, Müller WD, Schwitalla AD. The impact of different low-pressure plasma types on the physical, chemical and biological surface properties of PEEK. *Dent Mater* 2021;37:e15–22. <https://doi.org/10.1016/j.dental.2020.09.020>
- [5] Yu X, Ibrahim M, Liu Z, Yang H, Tan L, Yang K. Biofunctional Mg coating on PEEK for improving bioactivity. *Bioact Mater* 2018;3:139–43. <https://doi.org/10.1016/j.bioactmat.2018.01.007>
- [6] Przykaza K, Jurak M, Wiącek AE, Mroczyk R. Characteristics of hybrid chitosan/phospholipid-sterol, peptide coatings on plasma activated PEEK polymer. *Mater Sci Eng C* 2021;120. <https://doi.org/10.1016/j.msec.2020.111658>
- [7] Xu X, Li YY, Wang LL, Li YY, Pan J, Fu X, et al. Triple-functional polyetheretherketone surface with enhanced bacteriostasis and anti-inflammatory and osseointegrative properties for implant application. *Biomaterials* 2019;212:98–114. <https://doi.org/10.1016/j.biomaterials.2019.05.014>
- [8] Han X, Sharma N, Xu Z, Scheideler L, Geis-Gerstorfer J, Rupp F, et al. An in vitro study of osteoblast response on fused-filament fabrication 3D Printed PEEK for dental and cranio-maxillofacial implants. *J Clin Med* 2019;8. <https://doi.org/10.3390/jcm8060771>
- [9] Novotna Z, Reznickova A, Rimpelova S, Vesely M, Kolska Z, Svorcik V. Tailoring of PEEK bioactivity for improved cell interaction: plasma treatment in action. *RSC Adv* 2015;5:41428–36. <https://doi.org/10.1039/C5RA03861H>
- [10] Younis M, Unkovskiy A, ElAyouti A, Geis-Gerstorfer J, Spintzyk S. The effect of various plasma gases on the shear bond strength between unfilled polyetheretherketone (PEEK) and veneering composite following artificial aging. *Materials* 2019;12. <https://doi.org/10.3390/ma12091447>
- [11] Khoury J, Selezneva I, Pestov S, Tarassov V, Ermakov A, Mikheev A, et al. Surface bioactivation of PEEK by neutral atom beam technology. *Bioact Mater* 2019;4:132–41. <https://doi.org/10.1016/j.bioactmat.2019.02.001>
- [12] Han X, Yang D, Yang C, Spintzyk S, Scheideler L, Li P, et al. Carbon fiber reinforced PEEK composites based on 3D-printing technology for orthopedic and dental applications. *J Clin Med* 2019;8. <https://doi.org/10.3390/jcm8020240>
- [13] Wang H, Lu T, Meng F, Zhu H, Liu X. Enhanced osteoblast responses to poly ether ether ketone surface modified by water plasma immersion ion implantation. *Colloids Surf B Biointerfaces* 2014;117:89–97. <https://doi.org/10.1016/j.colsurfb.2014.02.019>
- [14] Wan T, Jiao Z, Guo M, Wang Z, Wan Y, Lin K, et al. Gaseous sulfur trioxide induced controllable sulfonation promoting biomineralization and osseointegration of polyetheretherketone implants. *Bioact Mater* 2020;5:1004–17. <https://doi.org/10.1016/j.bioactmat.2020.06.011>

- [15] Olivares-Navarrete R, Hyzy SL, Slosar PJ, Schneider JM, Schwartz Z, Boyan BD. Implant materials generate different peri-implant inflammatory factors: poly-ether-ether-ketone promotes fibrosis and microtextured titanium promotes osteogenic factors. *Spine* 2015;40:399–404. <https://doi.org/10.1097/BRS.0000000000000778>
- [16] Ren Y, Sikder P, Lin B, Bhaduri SB. Microwave assisted coating of bioactive amorphous magnesium phosphate (AMP) on polyetheretherketone (PEEK). *Mater Sci Eng C* 2018;85:107–13. <https://doi.org/10.1016/j.msec.2017.12.025>
- [17] Yuan B, Cheng Q, Zhao R, Zhu X, Yang X, Yang X. Biomaterials comparison of osteointegration property between PEKK and PEEK: Effects of surface structure and chemistry. *Biomaterials* 2018;170:116–26. <https://doi.org/10.1016/j.biomaterials.2018.04.014>
- [18] Torstrick FB, Lin ASP, Potter D, Safranski DL, Sulchek TA, Gall K, et al. Porous PEEK improves the bone-implant interface compared to plasma-sprayed titanium coating on PEEK. *Biomaterials* 2018;185:106–16. <https://doi.org/10.1016/j.biomaterials.2018.09.009>
- [19] Su Y, He J, Jiang N, Zhang H, Wang L, Liu X, et al. Additively-manufactured poly-ether-ether-ketone (PEEK) lattice scaffolds with uniform microporous architectures for enhanced cellular response and soft tissue adhesion. *Mater Des* 2020;191. <https://doi.org/10.1016/j.matdes.2020.108671>
- [20] Barkarmo S, Wennerberg A, Hoffman M, Kjellin P, Breeding K, Handa P, et al. Nano-hydroxyapatite-coated PEEK implants: A pilot study in rabbit bone. *J Biomed Mater Res Part A* 2013;101:465–71. <https://doi.org/10.1002/jbm.a.34358>
- [21] Lee JH, Jang HL, Lee KM, Baek H-R, Jin K, Hong KS, et al. In vitro and in vivo evaluation of the bioactivity of hydroxyapatite-coated polyetheretherketone biocomposites created by cold spray technology. *Acta Biomater* 2013;9:6177–87. <https://doi.org/10.1016/j.actbio.2012.11.030>
- [22] Ma R, Tang T. Current strategies to improve the bioactivity of PEEK. *Int J Mol Sci* 2014;15:5426–45. <https://doi.org/10.3390/ijms15045426>
- [23] Almasi D, Iqbal N, Sadeghi M, Sudin I, Abdul Kadir MR, Kamarul T. Preparation methods for improving PEEK's bioactivity for orthopedic and dental application: a review. *Int J Biomater* 2016;2016. <https://doi.org/10.1155/2016/8202653>
- [24] Liu C, Bai J, Wang Y, Chen L, Wang D, Ni S, et al. The effects of three cold plasma treatments on the osteogenic activity and antibacterial property of PEEK. *Dent Mater* 2021;37:81–93. <https://doi.org/10.1016/j.dental.2020.10.007>
- [25] Xu A, Liu X, Gao X, Deng F, Deng Y, Wei S. Enhancement of osteogenesis on micro/nano-topographical carbon fiber-reinforced polyetheretherketone-nanohydroxyapatite biocomposite. *Mater Sci Eng C* 2015;48:592–8. <https://doi.org/10.1016/j.msec.2014.12.061>
- [26] Waser-Althaus J, Salamon A, Waser M, Padeste C, Kreutzer M, Pielele U, et al. Differentiation of human mesenchymal stem cells on plasma-treated polyetheretherketone. *J Mater Sci Mater Med* 2014;25:515–25. <https://doi.org/10.1007/s10856-013-5072-5>
- [27] Bose S, Ke D, Sahasrabudhe H, Bandyopadhyay A. Additive manufacturing of biomaterials. *Prog Mater Sci* 2018;93:45–111. <https://doi.org/10.1016/j.pmatsci.2017.08.003>
- [28] Ngo TD, Kashani A, Imbalzano G, Nguyen KTQ, Hui D. Additive manufacturing (3D printing): a review of materials, methods, applications and challenges. *Compos Part B Eng* 2018;143:172–96. <https://doi.org/10.1016/j.compositesb.2018.02.012>
- [29] Kang J, Wang L, Yang C, Wang L, Yi C, He J, et al. Custom design and biomechanical analysis of 3D-printed PEEK rib prostheses. *Biomech Model Mechanobiol* 2018;17:1083–92. <https://doi.org/10.1007/s10237-018-1015-x>
- [30] Wang L, Huang L, Li X, Zhong D, Li D, Cao T, et al. Three-dimensional printing PEEK implant: a novel choice for the reconstruction of chest wall defect. *Ann Thorac Surg* 2019;107:921–8. <https://doi.org/10.1016/j.athoracsur.2018.09.044>
- [31] Honigmann P, Sharma N, Schumacher R, Rueegg J, Haefeli M, Thieringer F. In-hospital 3D printed scaphoid prosthesis using medical-grade polyetheretherketone (PEEK) biomaterial. *Biomed Res Int* 2021;2021. <https://doi.org/10.1155/2021/1301028>
- [32] Basgul C, Spece H, Sharma N, Thieringer FM, Kurtz SM. Structure, properties, and bioactivity of 3D printed PAEKs for implant applications: a systematic review. *J Biomed Mater Res - Part B Appl Biomater* 2021;109:1924–41. <https://doi.org/10.1002/jbm.b.34845>
- [33] Sharma N, Aghlmandi S, Dalcanale F, Seiler D, Zeilhofer HF, Honigmann P, et al. Quantitative assessment of point-of-care 3D-printed patient-specific polyetheretherketone (PEEK) cranial implants. *Int J Mol Sci* 2021;22:1–19. <https://doi.org/10.3390/ijms22168521>
- [34] Arif MF, Kumar S, Varadarajan KM, Cantwell WJ. Performance of biocompatible PEEK processed by fused deposition additive manufacturing. *Mater Des* 2018;146:249–59. <https://doi.org/10.1016/j.matdes.2018.03.015>
- [35] Xu Y, Unkovskiy A, Klau F, Rupp F, Geis-Gerstorfer J, Spintzyk S, et al. Compatibility of a silicone impression/adhesive system to FDM-printed tray materials—a laboratory peel-off study. *Materials* 2018;11. <https://doi.org/10.3390/ma11101905>
- [36] Rochford ETJ, Subbiahdoss G, Moriarty TF, Poulsson AHC, Van Der Mei HC, Busscher HJ, et al. An in vitro investigation of bacteria-osteoblast competition on oxygen plasma-modified PEEK. *J Biomed Mater Res - Part A* 2014;102:4427–34. <https://doi.org/10.1002/jbm.a.35130>
- [37] Rochford ETJJ, Poulsson AHCC, Salavarieta Varela J, Lezuo P, Richards RG, Moriarty TF. Bacterial adhesion to orthopaedic implant materials and a novel oxygen plasma modified PEEK surface. *Colloids Surf B Biointerfaces* 2014;113:213–22. <https://doi.org/10.1016/j.colsurfb.2013.09.012>
- [38] Zheng Y, Liu L, Ma Y, Xiao L, Liu Y. Enhanced osteoblasts responses to surface-sulfonated polyetheretherketone via a single-step ultraviolet-initiated graft polymerization. *Ind Eng Chem Res* 2018;57:10403–10. <https://doi.org/10.1021/acs.iecr.8b02158>
- [39] Rupp F, Gittens RA, Scheideler L, Marmur A, Boyan BD, Schwartz Z, et al. A review on the wettability of dental implant surfaces I: Theoretical and experimental aspects. *Acta Biomater* 2014;10:2894–906. <https://doi.org/10.1016/j.actbio.2014.02.040>
- [40] Wakelin EA, Yeo GC, Mckenzie DR, Bilek MMM, Weiss AS. Plasma ion implantation enabled bio-functionalization of PEEK improves osteoblastic activity. *APL Bioeng* 2018;2. <https://doi.org/10.1063/1.5010346>
- [41] Sundriyal P, Sahu M, Prakash O, Bhattacharya S. Long-term surface modification of PEEK polymer using plasma and PEG silane treatment. *Surf Interfaces* 2021;25:101253. <https://doi.org/10.1016/j.surfint.2021.101253>
- [42] Schwitalla AD, Bötzel F, Zimmermann T, Sütel M, Müller WD. The impact of argon/oxygen low-pressure plasma on shear bond strength between a veneering composite and different PEEK materials. *Dent Mater* 2017;33:990–4. <https://doi.org/10.1016/j.dental.2017.06.003>
- [43] Bötzel F, Zimmermann T, Sütel M, Müller WD, Schwitalla AD. Influence of different low-pressure plasma process parameters on shear bond strength between veneering composites and PEEK materials. *Dent Mater* 2018;34:e246–54. <https://doi.org/10.1016/j.dental.2018.06.004>

- [44] Zhang S, Awaja F, James N, McKenzie DR, Ruys AJ. Autohesion of plasma treated semi-crystalline PEEK: Comparative study of argon, nitrogen and oxygen treatments. *Colloids Surf A Physicochem Eng Asp* 2011;374:88–95. <https://doi.org/10.1016/j.colsurfa.2010.11.013>
- [45] Wu Y, Zitelli JP, TenHuisen KS, Yu X, Libera MR. Differential response of Staphylococci and osteoblasts to varying titanium surface roughness. *Biomaterials* 2011;32:951–60. <https://doi.org/10.1016/j.biomaterials.2010.10.001>
- [46] Deng Y, Liu X, Xu A, Wang L, Luo Z, Zheng Y, et al. Effect of surface roughness on osteogenesis in vitro and osseointegration in vivo of carbon fiber-reinforced polyetheretherketone– Nanohydroxyapatite composite. *Int J Nanomed* 2015;10:1425–47. <https://doi.org/10.2147/IJN.S75557>
- [47] Zhang W, Wang G, Liu Y, Zhao X, Zou D, Zhu C, et al. The synergistic effect of hierarchical micro / nano-topography and bioactive ions for enhanced osseointegration. *Biomaterials* 2013;34:3184–95. <https://doi.org/10.1016/j.biomaterials.2013.01.008>
- [48] Liang L, Krieg P, Rupp F, Kimmerle-Müller E, Spintzyk S, Richter M, et al. Osteoblast response to different UVA-activated anatase implant coatings. *Adv Mater Interfaces* 2018;6. <https://doi.org/10.1002/admi.201801720>